Indian Journal of Pure & Applied Physics
Vol. 27, July-August 1989, pp. 322-330

Three-site solar wind observatory

S K Alurkar, A D Bobra, N S Nirman, P Venat & P Jañardhan
Physical Research Laboratory, Ahmedabad 380 009

Radio astronomers at the Physical Research Laboratory, Ahmedabad, have exploited the well known phenomenon of interplanetary scintillation (IPS) which is observed using a ground-based radio astronomy technique. Three large radio telescopes operating at 103 MHz have been located at Thaltej near Ahmedabad, Rajkot and Surat in the State of Gujarat for the measurement of solar wind velocity. Details of indigenous design and development of various sub-systems which form the essential parts of the radio telescope are presented. These include a large antenna array, low noise pre-amplifiers, multi-beam-forming matrices, a correlation receiver and digital data acquisition and recording systems. Preliminary specimen results are presented and a brief account of the new scientific programmes and corresponding expansion of the Thaltej radio telescope are given.

1 Introduction

As a consequence of a series of the Pioneer spacecraft observations in the late 1960's, it became evident that the heliosphere near the earth's orbit is highly structured and that it is essentially three-dimensional as well as time varying. More recently, therefore, studies of the plasma density distribution and dynamics in the interplanetary medium (IPM) over a wide range of heliocentric distances up to the earth's orbit and beyond, as well as over a wide range of helio-latitudes have assumed importance. Both ground-based techniques and space platforms are used in studying the solar wind plasma. Space probes make in situ measurements of the solar plasma parameters, while the ground-based instruments measure values of the parameters averaged along the line-of-sight to the source of radiation.

In addition to the interplanetary travelling shockwaves, long lived high speed plasma streams originating from polar coronal holes exist in the IPM. Studies of spatial and temporal evolutions of such plasma streams are important in understanding the distribution and generation of inhomogeneities of plasma density in the heliosphere. The present three-telescope system will be very suitable for making 3-dimensional studies of these large-scale structures using a grid of a large number of scintillating radio sources around the sun.

The experiment makes use of the well known phenomenon of Interplanetary Scintillation (IPS) which is observed with the ground-based technique of radio astronomy. To study the micro-scale structure (about 10^2-10^3 km) of plasma density inhomogeneities and their movement in the interplanetary medium, a system of three large radio telescopes is developed. The telescopes operate at 103 MHz and are situated at Thaltej, near Ahmedabad, Rajkot and Surat in the Gujarat State. This IPS technique of estimating the velocity of the solar plasma has an edge over in situ measurements by spacecraft in that it enables the velocity measurements not only in the ecliptic plane, but also at more interesting higher ecliptic latitudes which are as yet inaccessible to spacecraft.

2 The Phenomenon of IPS

The phenomenon of interplanetary scintillation is a radio analogy of the twinkling of stars in the night sky and atmospheric scintillation of laser

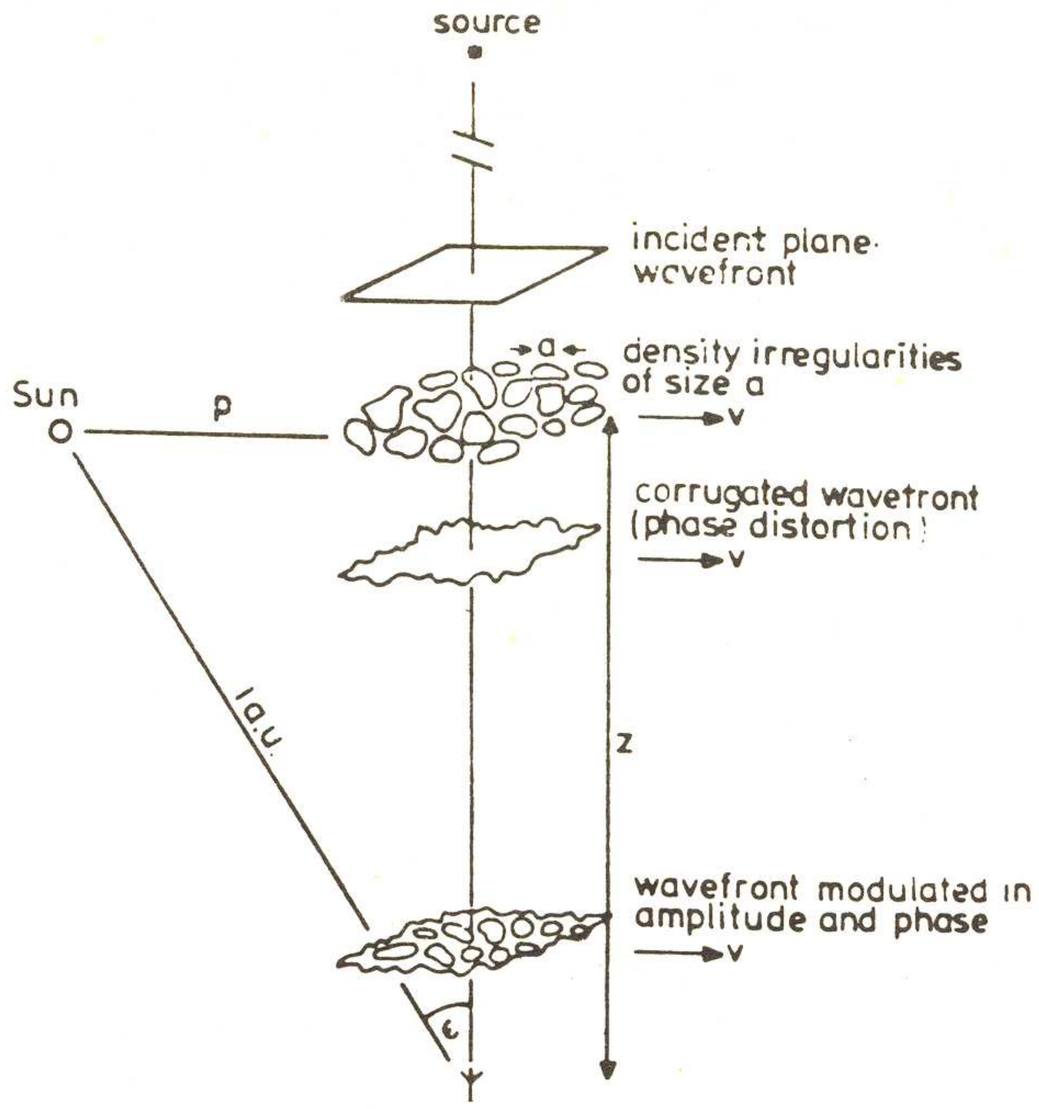

Fig. 1 – The phenomenon of interplanetary scintillation

beams. As sketched in Fig. 1, when radio waves from a distant compact source enter the interplanetary medium containing solar plasma, they are scattered by the irregularities of refractive index of the plasma. If the radio source is sufficiently small in diameter so that the plasma density irregularities are illuminated coherently, phase deviations are imposed on the plane wavefront. Emerging out from the scattering medium, these phase-deviated waves propagate in the IPM and interfere with one another, causing at the earth fluctuations of intensity of the radio source. As a result of the solar wind flow across the line-of-sight, the spatial distribution of plasma density variation in the scattering medium is converted into temporal fluctuations of the intensity at the observer with a typical period of one second.

Thus, the IPS method provides essentially a one-dimensional scan of the scattering region. Radio sources with angular sizes of about 1.0 arcsecond or less cause IPS yielding a temporal spectrum ranging from 0.1 to 3 Hz. The scintillators are mainly extragalactic radio sources, such as quasars, a fraction or whole of which is effective as a scintillating radio source.

2.1 Brief Theory of IPS

The IPS geometry is shown in Fig. 2. The density irregularities are convected radially outwards in a spherically symmetric medium with a velocity V.

At the observer's plane $z = z_0$, the drifting intensity pattern is characterized by the 2-D spatial spectrum of intensity[1,2]

$M_{2I}(k_x, k_y)$ where $k = (k_x^2 + k_y^2)^{1/2}$ ... (1)

is the spatial wavenumber. Scintillation index m is defined as:

$$m^2 = \int\int M_{2I}(k_x, k_y)\, dk_x\, dk_y \quad \ldots (2)$$

Temporal spectrum $P(f)$ is given by:

$$P(f) = 4/V_T \int M_{2I}(k_x = 2\pi f/V_T, k_y)\, dk_y \quad \ldots (3)$$

where f = frequency of the radio waves from the source and V_T is the component of V transverse to the line-of-sight. The moments of this spectrum are given by:

$$f_n = \int_{-\infty}^{\infty} f^n P(f)\, df \Big/ \int_{-\infty}^{\infty} P(f)\, df \quad \ldots (4)$$

which are related to the statistics of the random medium as shown below.

The scattering medium is characterized by the 3-D spatial spectrum of electron density fluctuations $M_{3N}(k_x, k_y, k_z)$ in the solar wind plasma, so that the integral of M_{3N} equals the total mean square fluctuation $\langle \delta N^2 \rangle$.

A thin layer of thickness dz imposes on the incident wave of wavelength λ a 2-D spectrum of phase fluctuations:

$$M_{2\phi}(k_x, k_y) = 2\pi\lambda^2 r_e^2 \cdot M_{3N}(k_x, k_y, k_z = 0)\, dz \quad \ldots (5)$$

wnere r_e = classical electron radius.

$$\int\int M_{2\phi}(k_x, k_y)\, dk_x\, dk_y = \beta(r) \quad \ldots (6)$$

is the mean square deviation imposed on the wave and is called the scattering power. The total mean square phase deviation for uncorrelated irregularities between successive layers is:

$\phi_0^2 = \int_{-\infty}^{z_0} \beta(r)\, dz$ from the source to the observer.

The relation between the 2-dimensional intensity spectrum $M_{2I}(k_x, k_y)$ and $M_{3N}(k_x, k_y, k_z)$ depends on the value of ϕ_0^2. For $\phi_0^2 << 1$, i.e. the weak scattering case, interpretation of scintillation observations is straightforward. For $\phi_0^2 >> 1$, i.e. the strong scattering condition, the relation is quite complicated. For $\phi_0^2 << 1$, M_{2I} and the properties of the medium and source are related through

$$M_{2I}(k_x, k_y) = M_{2\phi}(k_x, k_y, r) \cdot F(k_x, k_y, \lambda z_1) \, V^2(k_x, k_y, \theta_0, z_1)\, dz \quad \ldots (7)$$

where $z_1 = z - z_0$ = distance between the layer and observer and $F = 4 \sin^2(k^2\lambda z_1/4\pi)$ = Fresnel filter function. V^2 = square of source visibility function which is related to source brightness distribution, $B(\theta)$.

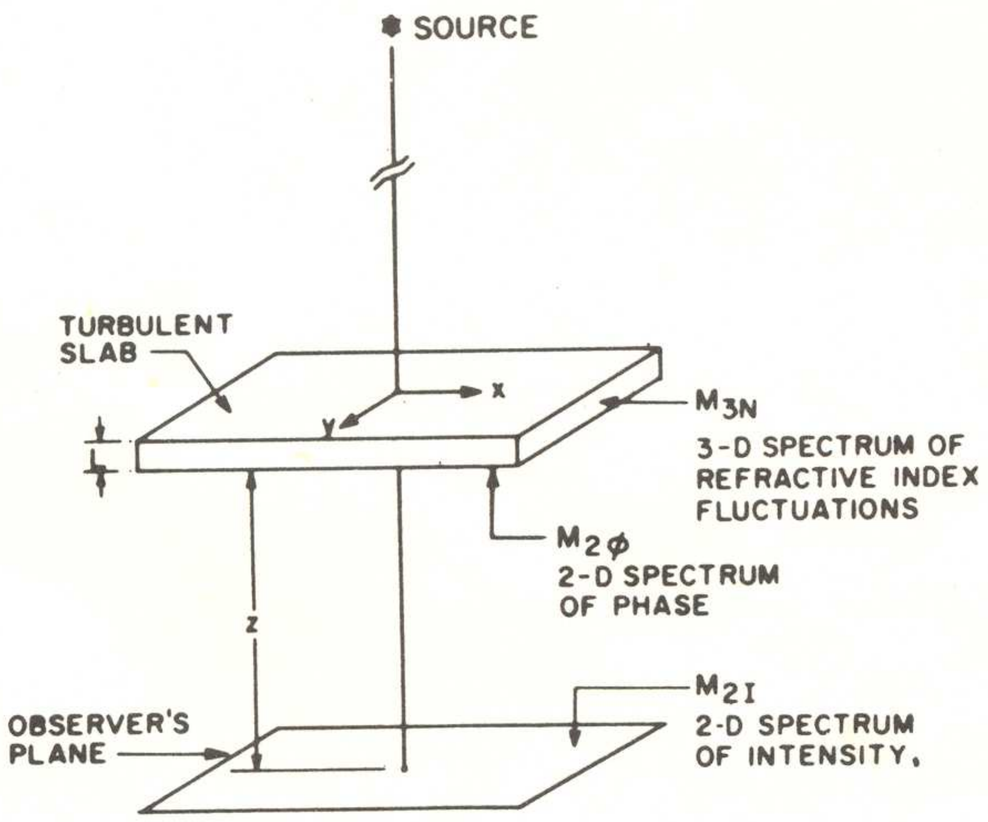

Fig. 2 – Formation of IPS spectrum

3 Basic Considerations for the Design of IPS Telescope

The design of the IPS telescope was based on the following important features:

(a) Frequency of operation and (b) Size and site for telescope.

3.1 Frequency of Operation

The principal consideration for the choice of the operating frequency of a radio telescope depends upon the scientific information one wants to extract. At VHF frequencies, reliable IPS observations can be made over a solar elongation range of about 0.2 to 1.2 AU.

The sensitivity, or minimum detectable flux of a scintillating source, of a radio telescope to scintillations is given by[3]

$$\Delta S_{\min} = K \frac{T_N}{\eta A} \left(\frac{\Delta \nu_1 \Delta \nu_2}{\Delta \nu_{HF}^2} \right) 1/2 \quad \ldots (8)$$

where K = receiver constant near unity, T_N = noise temperature of the system, k = Boltzmann's constant = 1.38×10^{-23} JK^{-1}, ηA = effective collecting area of the antenna, $\Delta \nu_{HF}$ = HF bandwidth, $\Delta \nu_1$ = post-detector bandwidth and $\Delta \nu_2$ = scintillometer bandwidth. Now, the scintillation index $m = \frac{\Delta S}{\langle S \rangle}$, where $\langle S \rangle$ = mean flux density of the radio source. Thus, $m_{\min} \propto T_N \cdot (\eta A)^{-1} \cdot \langle S \rangle^{-1}$.

In the VHF band, the system noise temperature is governed mostly by the galactic background radiation, which varies with frequency as $T_N \propto \nu^{-2.55}$.

The effective area of a telescope is proportional to its geometrical area, which for a given number of dipoles, is given as $(\eta A) \propto \nu^{-2}$. Otherwise, it is independent of frequency.

The flux density of a typical radio source is given by $S \propto \nu^{-0.75}$.

The scattering properties of the interplanetary medium depend on frequency. In weak scattering and for Gaussian irregularity spectrum, the observed S.I. obeys the relation $m \propto \nu^{-1}$. Putting these relations together yields:

$$m_{\min} \propto \nu^{-2.55} \cdot \nu^2 \cdot \nu^{0.25} \cdot \nu^{7.0} \propto \nu^{1.2} \quad \ldots (9)$$

This relation shows that to maximise the sensitivity of the radio telescope to scintillations, as low a frequency as possible should be chosen. But some other factors must also be considered. These are (i) ionospheric scintillations increase rapidly with decreasing frequency until the ionosphere becomes opaque when $\nu \sim 10$ MHz, (ii) long-range ducted interference increases with decreasing frequency and (iii) the value of m increases with decreasing solar elongation (the sun-earth-source angle) until it saturates when the scattering becomes stronger, after which it decreases to zero.

Thus, a frequency in the range 80-120 MHz is appropriate for IPS studies of interplanetary transients.

3.2 Size and Site of Telescope

The choice of the aperture of the IPS antenna array was made on the basis of the scientific objectives aimed at. For studying density structure and dynamics of the solar wind over a range of ecliptic latitudes and solar elongation, it is necessary to observe a good number of scintillating radio sources around the sun. It was proposed to observe some 25 sources round the year with an antenna aperture of about 5000 sq. m at 103 MHz.

In addition, the antenna aperture of the Thaltej telescope has been doubled to 10,000 sq.m. IPS observations of a number of compact radio sources, such as quasars, made using a single large radio telescope are used to compute IPS spectra and scintillation indices (a measure of turbulence in the solar plasma) which, in turn, are useful in deriving the distribution of plasma density irregularities and mapping of plasma turbulence in the IPM and angular size of scintillating radio sources. Only radio sources with angular size in the range 0.1-1 arcsecond exhibit IPS.

To get meaningful IPS data from each of the three telescopes, these must be situated at places with acceptable electrical interference level. Also for satisfactory cross-correlation of IPS data, the telescopes should be separated from one another by a distance comparable to the first Fresnel zone size. The IPS telescopes are installed at Thaltej about 6 km from Ahmedabad, in Saurashtra University Campus, Rajkot and in the South Gujarat University Campus, Surat forming a triangle with baselines of about 200 km each (Fig. 3).

The geographic coordinates of the sites are presented in Table 1.

4 Interferometeric Layout of the Antenna Array at Thaltej

The antenna array is split up in two parts in the N-S direction, each consisting of 32 EW rows of 32 dipoles each. Each group of 32 rows, after preamplification, is followed by a 32-element multibeam-forming matrix, called Butler Matrix. The amplified RF signals at 103 MHz are carried to the matrices through underground coaxial cables.

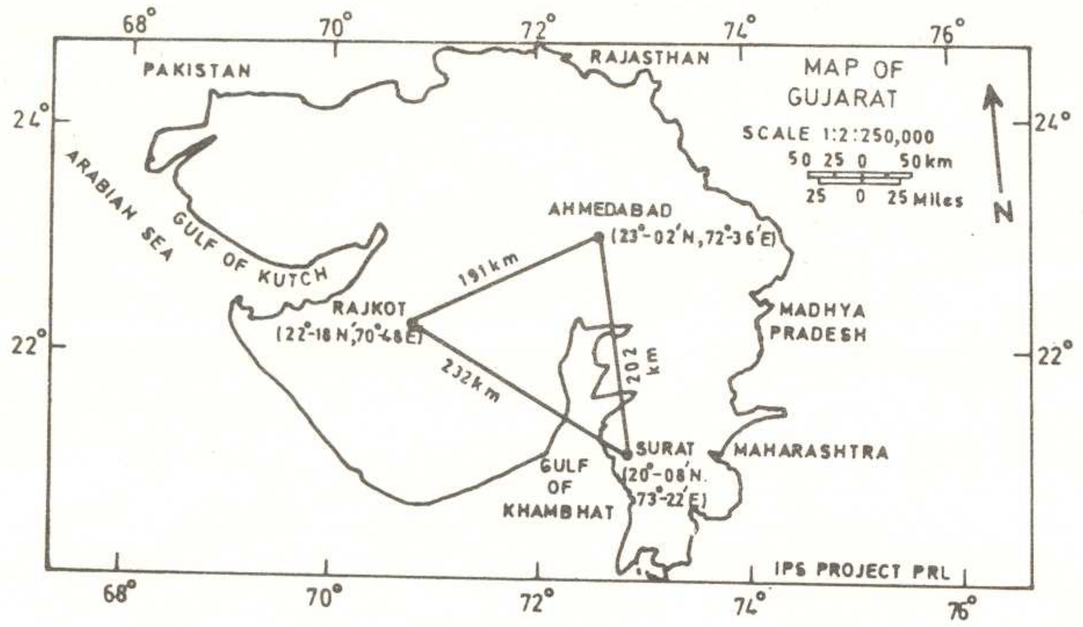

Fig. 3 – Geometry of the three IPS sites

Table 1 – Geographic coordinates of the IPS sites

	Thaltej	Rajkot	Surat
Longitude	72°29′38.86″E	70°44′26.58″E	72°47′05.05″E
Latitude	23°02′39.48″N	22°17′28.82″N	21°09′05.05″N

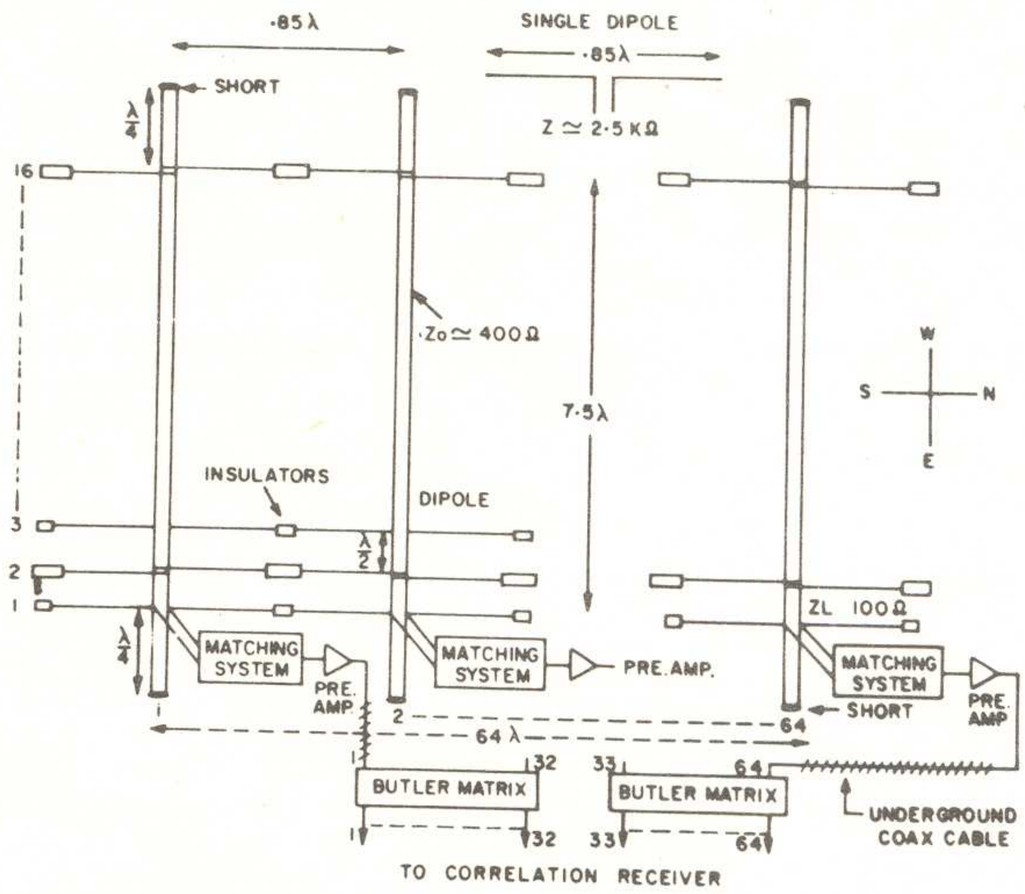

Fig. 4 – Schematic of IPS antenna array and correlation receiver system

The schematic diagram of the array is shown in Fig. 4. The antenna aperture is thus divided into two halves, with each half giving a pattern of 32 beams deployed in declination. For the 10,000 sq.m antenna at Thaltej the size of each beam at the zenith is about 3.6° EW × 1.8° NS. The variation of the beam size in right ascension (RA) and declination is given by 3.6° sec δ and 1.8° sec $(23° - \delta)$, where δ is the declination of the beam and 23° is the approximate latitude of Thaltej[4].

5 Pre-amplifiers and Multibeam-forming Matrix

In order to realise the maximum aperture sensitivity of the antenna array, low noise pre-amplifiers were introduced immediately after the impedance matching baluns connected to the antenna. Near 103 MHz, the equivalent noise temperature of the galactic background is about a few thousand degrees Kelvin. This is generally much larger than the noise temperature of receivers at VHF. Thus, the system noise temperature is given by:

$$T_{sys} = T_{sky} + T_R \;,\; T_R = (N-1)\,T_0 \qquad \ldots (10)$$

where T_{sky} = equivalent noise temperature of galactic background, T_R = noise temperature of receiver, N = noise factor of the pre-amplifier and T_0 = ambient temperature of the receiver. T_{sys} is mainly decided by the galactic background[5]. The sensitivity of the receiver, in turn, becomes sky noise limited. The pre-amplifiers, with an average noise factor of 2 or less, were designed such that they selectively amplify the 103 MHz signals and compensate for the attenuation through the coaxial cables connecting the receiver. Another important feature of the pre-amplifiers is their phase stability. The amplified RF signals are fed into a multibeam-forming matrix. The accuracy of its beam formation depends on the phase and gain stability of the pre-amplifiers. For good long-term phase stability, the bandwidth of an amplifier should be sufficiently large. Their average bandwidth was 7 MHz.

To simplify observational procedure of IPS of a number of radio sources, it was decided to operate the telescopes as transit instruments. Thus, a steady multibeam pattern can be formed using a beam-forming network. Apart from the ease of operation, the multibeam pattern enables simultaneous scanning of a number of equispaced strips of the sky when equal number of receivers are used. In the case of the IPS telescopes, the beams are formed in declinations. Such a multistrip scanning telescope would be particularly suitable for radio sky surveys, study of heliospheric disturbances[6], using the technique of 'g-maps' of plasma turbulence[7].

Each of the IPS telescopes works as a correlation interferometer in conjunction with a correlation receiver so that its output is proportional to the time-averaged product of the voltages from the North and South halves of the antenna. Such a receiver is insensitive to most of the undesirable noise which contributes to the uncorrelated voltage components received from the two parts of the antenna, whose time-averaged product tends to zero.

6 Low-noise Pre-amplifier

In Fig. 4 is shown the schematic arrangement of the antenna array with low noise pre-amplifiers (LNA) and two multibeam-forming matrices. The

Table 2 – Important characteristics of the pre-amplifier

Centre Frequency	103 MHz
Bandwidth (– 3 dB)	7 MHz average
Gain	30 to 40 dB
Noise figure	3 dB average
Input and output impedance	55 to 60 ohm ± 3 pF

103 MHz signal from each EW row of the antenna array is enhanced by a 3-stage LNA of the cascade type. In the second stage, a gain-control is incorporated to equalize the relative gain and phase of all the amplifiers as measured from the receiver room. Some important features of the pre-amplifiers are given in Table 2.

7 Butler Matrix

After amplification, the RF signal is carried through underground coaxial cables to the BMs situated inside the receiver hut. This ensured phase and amplitude stability of the signal to within ± 1.5° and ± 0.5 dB respectively.

It generates simultaneous independent beams from identical outputs of an antenna array with a uniformly illuminated aperture[7]. A computer plot of the multibeam pattern in declination for a 32-element BM is shown in Fig. 5. The adjacent beams cross each other at – 4 dB points. At the wavelength of 2.91m and element-spacing of 0.85 wavelength, the angular coverage of the pattern in declination works out to about ± 30° around the zenith. The envelope of the beams has a cosine taper such that the 16th beam will be nearly 3 dB down with respect to the beams near the zenith.

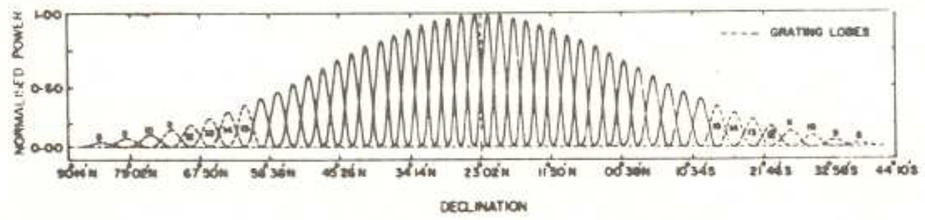

Fig. 5 – Multibeam power response of the Thaltej antenna array

It is well known that in the case of a transit antenna, grating lobes are formed due to foreshortening effect when the main lobe of the antenna is pointed in a direction far away from the zenith[4]. As shown in Fig. 5, grating lobes become important beyond the 12th beam on either side of the local zenith. IPS observations made with beams 10th (on either side of zenith) and beyond are, therefore, interpreted with caution.

8 Correlation Receiver

Fig. 6 shows a block diagram of the correlation receiver. It is a dual channel receiver (sin and cos) which is connected to the two halves of the antenna array to form a phase-switched interferometer in declination. The receiver has a common crystal-controlled local oscillator operating at 73 MHz, giving an IF of 30 MHz for each channel with a bandwidth of about 2.0 MHz.

In a correlation receiver, the IF output voltages from two identical channels are multiplied. As a result, time-averaged uncorrelated noise voltages produce zero dc voltage at the multiplier output. A compact radio source, however, produces correlated signal power equal to $(k \cdot \Delta T \cdot B)$ at the inputs of the two receivers and IF output voltages having amplitudes proportional to $(k \cdot \Delta T \cdot B)^{1/2}$, where k is the Boltzmann's constant, ΔT the change in noise

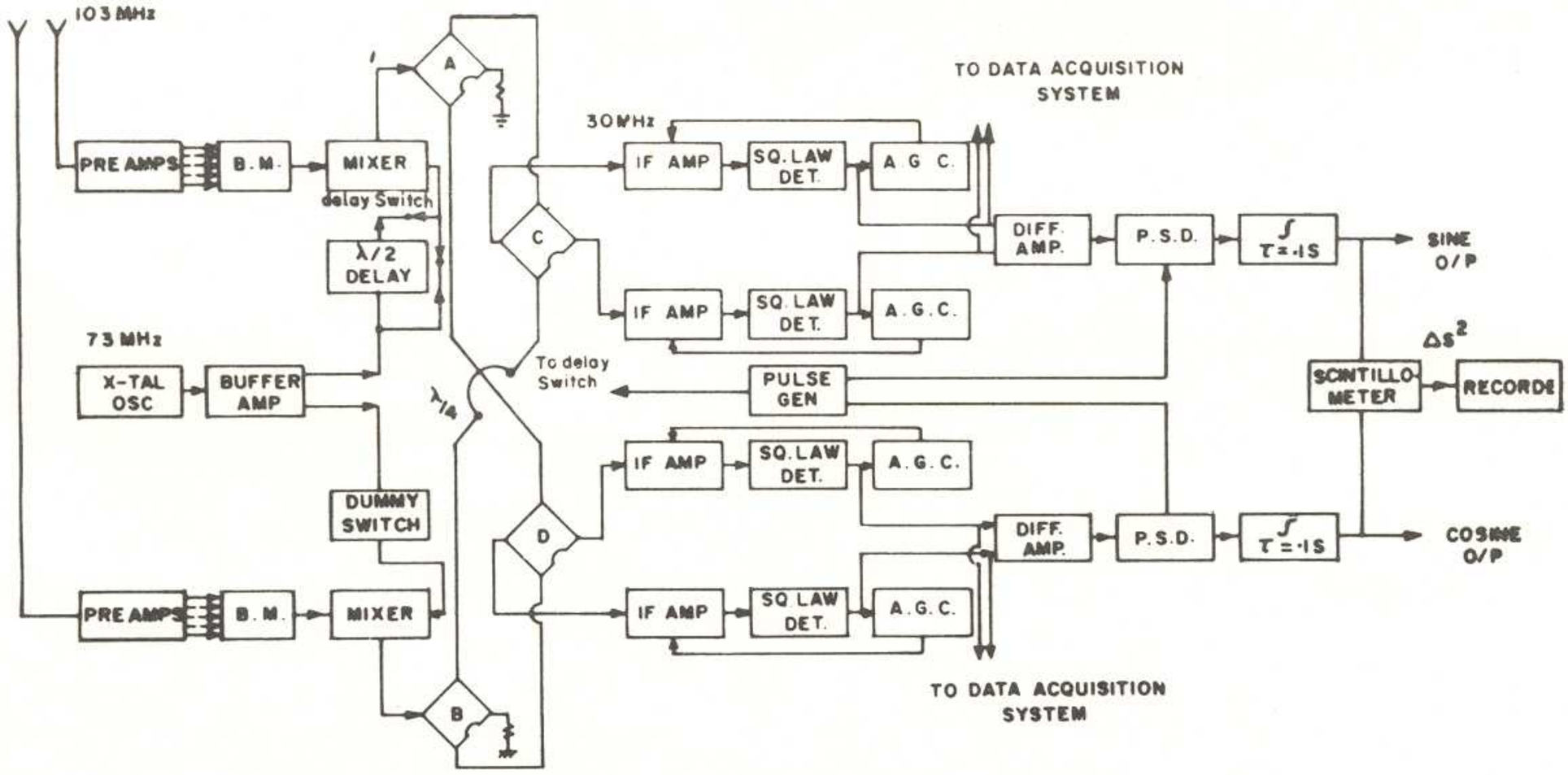

Fig. 6 – Block diagram of correlation receiver

temperature due to the source and B the pre-detection bandwidth. If ϕ is the phase angle between them, then the dc output voltage of the multiplier will be equal to $k \cdot \Delta T \cdot B \cdot \cos \phi$. The sensitivity of the correlation receiver is given by[5]

$$\Delta T_{\min} = \frac{1}{\sqrt{2} \cos \phi} \qquad \ldots (11)$$

$$\approx 4 \text{ K for } \phi = 0$$

where T_{sys} = system noise temperature of each receiver and τ = post-detection integration time-consant. Hence, the minimum detectable flux density becomes,

$$\Delta S_{\min} = \frac{2k\Delta T_{\min}}{A_e} \qquad \ldots (12)$$

where A_e is the effective antenna aperture.

For the Thaltej telescope, $\Delta S_{\min} \simeq 7\ J_y$, with S/N of 5, assuming antenna efficiency of 80 per cent. Signals from the two halves of the antenna array are brought to two 32-element beam-forming matrices BM-1 and BM-2. For a given source, signals from the corresponding beam ports are given to the inputs of the two receivers through low-noise pre-amplifiers of the type described earlier. A common local oscillator (73 MHz) feeds the two balanced mixers through a phase-switch. The outputs of the two mixers are each divided into two parts using coaxial hybrid rings A and B. One output signal each from A and B hybrids are combined in phase in the third hybrid D for 'cos' signals, while the second output from A is combined in the fourth hybrid C with the second output from B after a delay of 90°. The output of C, therefore, gives the 'sin' signals. Each of the two receiver channels has two 30 MHz intermediate frequency (IF) amplifiers with an average bandwidth of about 2.0 MHz. The outputs of these high gain (80 dB) IF amplifiers are maintained at a constant level within about 1 dB using automatic gain controls (AGCs) having a time constant of about 10 s. The characteristics of the square-law detectors are such that the AGC becomes effective without the antenna connected.

Low-pass filtering with time-constants of 0.1s is used after the phase-sensitive detectors (PSDs). This integration time-constant, therefore, allows intensity fluctuations at frequencies up to a limit of about 10 Hz. The effects of ionospheric scintillations, which are usually weak at tropical latitudes at a frequency of 103 MHz, when present, are prominent below about 0.1 Hz. The IPS data are, therefore, passed through a digital filter with a low frequency cut-off at 0.1 Hz before computing IPS spectra.

The square-law detector diodes are selected for similarity and are connected such that the output voltage remains within the square-law range of about 10 to 70 mV. The AGC is so adjusted that with the antenna connected and no source in the beam the square-law output remains below 45 mV.

For uncorrelated signals, the outputs of the difference amplifiers remain zero. Correlated signals produce output voltage at cos or sin channel or at both, depending on the relative phase of the input signals. This square-wave modulated signal at the switching frequency is converted to sine-wave by the active filter-circuit and phase-detected in synchronisation with the phase-switch. The sin and cos outputs are recorded on a chart recorder as well as on a digital tape recorder.

Some important parameters of the correlation receiver are presented in Table 3.

When a scintillating radio source is observed by a phase-switching interferometer, there appear three main components in its output. They are:

1 A broadband system noise voltage covering a frequency range from zero up to the higher cut-off determined by the receiver time constant.
2 A slowly-varying voltage due to the passage of the source through the interference pattern of the telescope. Its frequency spectrum depends on the dimensions and spacings of the antenna elements, with an upper limit given by $7.3 \times 10^{-5}\ (d/\lambda) \cos \delta$ Hz, where d is the east-west dimension, δ the declination and λ the wavelength[8]. For the IPS telescope with 5000 sq. m aperture, this works out to a maximum of about 6×10^{-4} Hz for $\delta = 0$.
3 A desirable rapidly changing voltage which is due to scintillations. It has a noise-like character and its frequency spectrum depends on the existing conditions in the solar wind, solar elongation, the apparent angular diameter of the source, the receiver bandwidth, etc.

The scintillating signals at the outputs of the sin and cos receivers may be expressed as[3]:

$$V_s = f(t) \cdot A \cdot \sin(bt) \cdot \frac{\sin^2(at)}{(at)^2} \qquad \ldots (13)$$

and

$$V_c = f(t) \cdot A \cdot \cos(bt) \cdot \frac{\sin^2(at)}{(at)^2} \qquad \ldots (14)$$

where $A \cdot \frac{\sin}{\cos}(bt) \cdot \frac{\sin^2(at)}{(at)^2}$ is the pattern of

Table 3 – Important parameters of correlation receiver

Item	Center frequency	(−3 dB) Bandwidth (MHz)	Input impedance (ohms)	AGC level		Suppression range of AGC		Gain (dB)
				N_0 I/P (V)	−60 dBm I/P (V)	I/P (dBm)	O/P (mV)	
Pre-amp 1	103.0	12.0	55 −j 1.5	—	—	—	—	25.0
Pre-amp 2	103.0	12.0	57 −j 2.0	—	—	—	—	25.0 (without AGC)
sin R_x								
IF 1	30.1	2.55	50 −j 2.0	−0.4	−1.3	−60	45.5	80.0
IF 2	30.0	2.50	52 −j 3.0	−0.5	−1.4	−60	45.5	80.0
cos R_x								
IF 1	30.0	2.50	51 −j 1.5	−0.44	−1.5	−60	49.0	80.0
IF 2	30.05	2.60	53 −j 2.0	−0.3	−1.2	−60	44.0	80.0
sin R_x								
IF 1	—	—	—	—	−2.4	−30	97.0	—
IF 2	—	—	—	—	−2.3	−30	85.0	—
cos R_x								
IF 1	—	—	—	—	−2.4	−30	95	—
IF 2	—	—	—	—	−2.0	−30	83	—

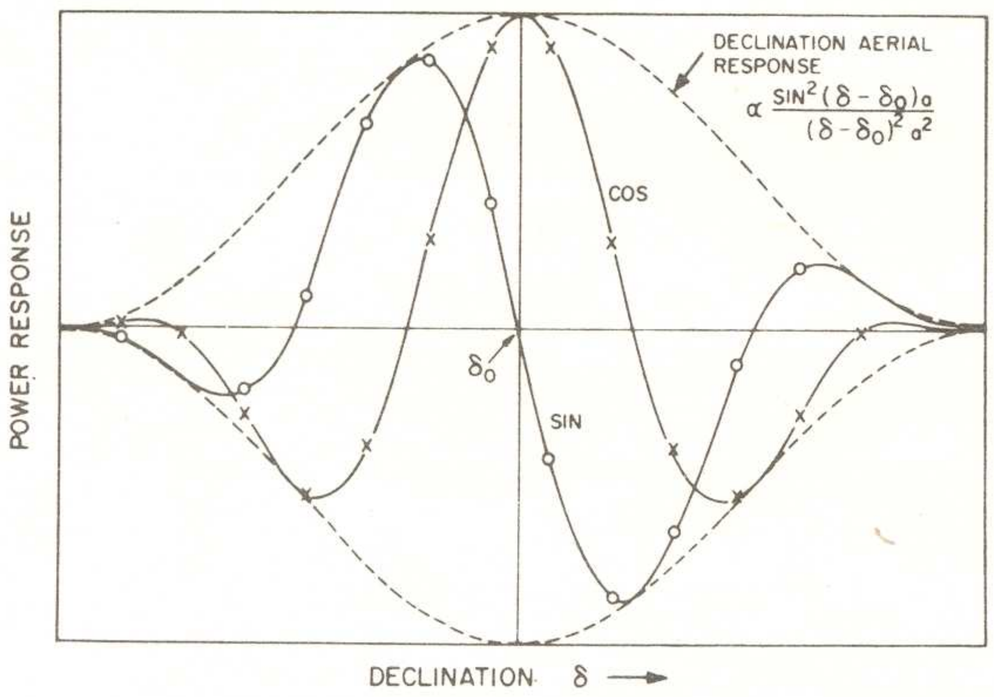

Fig. 7 – sin and cos fringes of correlation interferometer

this slowly-varying voltage and the function $f(t)$ defines the temporal changes in its amplitude.

9 Correlation Interferometer Fringes

As mentioned earlier, the antenna array is divided into two halves, each half comprising 32 rows of dipoles. The interferometer operation is effected by multiplying the response of the southern half of the antenna aperture with its northern half. The resulting antenna response in declination, together with the sin and cos fringes of the correlation type receiver, are sketched in Fig. 7. The half power beamwidths of this aerial response near zenith are about 1.8° in declination and 3.6° in right ascension. Such an interferometer has an advantage that a radio source stays on the same sin and/or cos fringe during its transit.

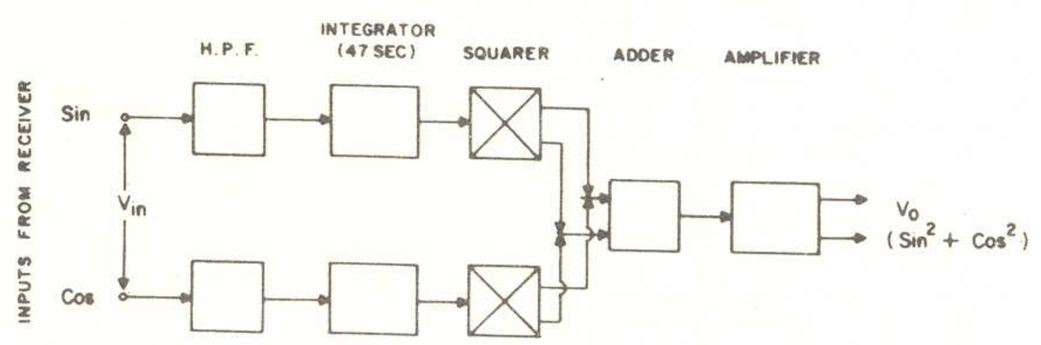

Fig. 8 – Block diagram of scintillometer

10 Scintillometer

The sin and cos signals are also fed to a scintillometer (Fig. 8). This unit squares the scintillating part of the two signals and adds them, averaging over a long time constant of 47 s. The scintillometer output shows a deflection proportional to the square of the scintillating flux, modulated by the square of the antenna pattern. The output is recorded on the third channel of the chart recorder along with the sin and cos signals.

The sensitivity of the scintillometer is expressed as[3]

$$(\Delta S)_{\min} = 4 \frac{kT_N}{A_e} \left(\frac{1}{\tau_1 \tau_2 \Delta f^2} \right)^{1/4} \quad \ldots (15)$$

where, ΔS = rms value of the scintillating flux density of the radio source, T_N = system noise temperature, A_e = effective antenna area, about 10,000 sq. m for the Thaltej telescope, $\tau_1 = 0.1$ s (time-constant of sin and cos integrators), $\tau_2 = 47$s (time-constant of scintillometer integration) and Δf = overall (−3 dB) bandwidth of the IF amplifiers (2 MHz).

For the Thaltej total power scintillometer connected to the phase-switching receiver, this sensitivity turns out to be about 1.0 Jansky rms (1 Jansky = 10^{-26} W m^{-2} Hz^{-1}).

11 Digital Data Acquisition System

The sin, cos and scintillometer analog outputs are recorded on a strip-chart. The sin and cos data are converted to digital form and simultaneously recorded on digital magnetic tapes for further processing and analysis.

The data available from the correlation receiver have a band-limited spectrum up to about 10 Hz (IPS spectrum lies between about 0.1 Hz to 10 Hz).

The simple data acquisition system (DAS)[8] was modified to suit the requirement of automatic data collection system. It was estimated that the number of sources which could be observed would not exceed about 250 and that normally a fixed sampling frequency of 20 Hz would be satisfactory. Also A/D converter should, if possible, have a higher resolution.

Fig. 9 shows a block diagram of the modified data acquisition system indicating most of the input/output (I/O) signals[9]. The system comprises source library, hex encoder, control circuit, A/D converter, data multiplexer, mux controller and pertec controller.

Th system keeps track of a sidereal clock (SDT) and decides about various observing schedules to be followed, to an accuracy of a minute. This avoids up-dating the transit time by 4 min every day. Once the SDT is stored for a source in the source library, it is unaltered throughout the observing session.

One of the most important jobs in the 3-station experiment is the 'time keeping' at the three sites. The relative time accuracy aimed at between a pair of IPS sites is ± 5 ms. The National Physical Laboratory, New Delhi, is maintaining a national time standard. This time standard, called ATA, is in the form of time pulses transmitted at 5, 10 and 15 MHz. The ionospheric delays between New Delhi and any of the three sites in favourable conditions[10] is about 4.0 ms. Thus, by using the ATA as a source of primary time standard for synchronisation, it is possible to achieve the required time accuracy.

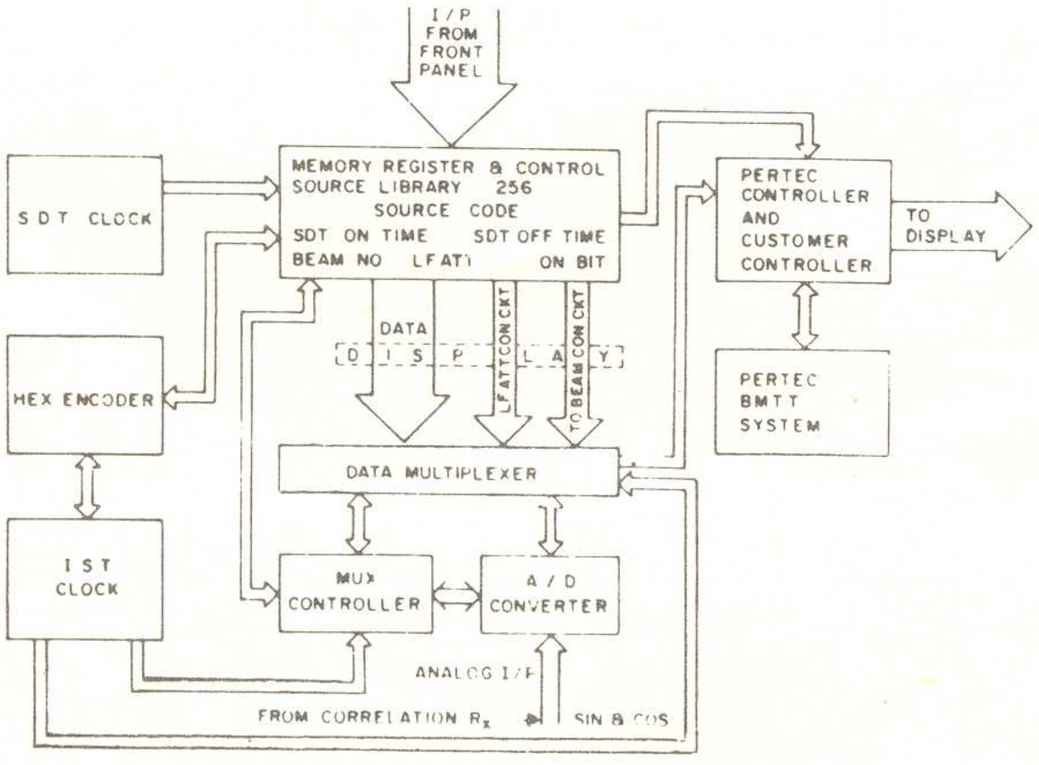

Fig. 9 – Automatic data acquisition system

12 Estimation of Solar Wind Velocity

In the IPS observations the measurable quantity is the temporal variations of intensity of a scintillating radio source. From the statistics of these intensity variations important parameters, such as, the scintillation index (S.I. = rms scintillating flux/mean source flux), scale size of pattern intensity variations, pattern velocity, etc. can be estimated. Under conditions of weak scattering, these parameters can be directly related to the corresponding quantities of the scattering medium.

The analysis of 3-site data is based on the assumption that the solar wind has a well-defined scale of velocity and that the diffraction pattern is 'frozen', drifting along the ground with the constant velocity[11,12]. It may be noted that a well-defined velocity scale implies a unique width or spatial scale of the wavenumber density irregularity spectrum. This is true only if the irregularity spectrum is Gaussian, but is not valid when the latter is a power law.

12.1 Basic considerations underlying the Cross-Correlation Analysis

The cross-correlation at a time lag Δt between two time series data of intensity measured at sites separated in the observing plane by a baseline of length $r(x,y)$ is expressed as[12]

$$C(r,\Delta t) = \langle I(r_0,t) \cdot I(r_0 + r, t + \Delta t)\rangle / \langle I^2\rangle \quad \ldots (16)$$

where $I(r_0,t)$ is the intensity measured at time t and location r_0 in the observer's plane normal to the line-of-sight. Since the mean intensity $\langle I\rangle$ is constant, the deviation $\delta I(r_0,t) = I(r_0,t) - \langle I\rangle$ is subjected to statistical analysis. The statistical averages of I are independent of the time over which they are averaged and are equal to the infinite time averages, which implies that the power spectrum of intensity does not vary with time.

The correlation function $C(r,\Delta t)$ contains information about the motion and scale sizes of the scattering inhomogeneities of plasma density. Any velocity contributing to the movement of the diffraction pattern is a function of wavenumber in

Table 4 – Preliminary estimates of solar wind velocity

Date	V_{pk} (km/s)	V_{mid} (km/s)	V_{perr} (km/s)	V_{merr} (km/s)
11.3.87	472	487	11	22
16.4.87	372	378	24	27
21.4.87	519	524	24	2
15.5.87	429	421	79	75
17.5.87	480	447	95	99
19.5.87	561	504	154	148
26.5.87	434	403	97	94
29.5.87	313	284	90	73
31.5.87	252	228	61	57

The last two columns give the rms errors inpeak and mid-velocities, V_{pk} and V_{mid}.

$$\text{theirregularityspectrum}\left(\text{wavenumber}\,k=\frac{2\pi}{\lambda_H}=\frac{\omega}{V}\right),$$

position in the scattering medium and time. The shape of the irregularity spectrum depends, among other things, on the velocity structure in the solar wind. Due to both the temporal smoothing required for estimating the correlation function and spatial smoothing effected by the scattering region (at 0.5 AU), the IPS technique cannot be used to study the velocity structures.

Velocity measurements at PRL, Ahmedabad, are made using cross-correlation analysis of intensities between the 3 pairs of sites Thaltej-Rajkot (191 km), Rajkot-Surat (232 km) and Surat-Thaltej (202 km).

Following the apparent velocity method[14], two estimates of the effective time taken by the intensity pattern to move from one antenna to the other are made; T_{pk} from the peak of the cross-correlation and T_{mid} from the mid-point at half the maximum correlation. The three values of each for the three baselines are combined to give two vector pattern velocities V_{pk} and V_{mid}. The difference $V = V_{pk} - V_{mid}$ gives the random velocity component.

Regular 3-site IPS observations were started in March 1987. First estimations of solar wind velocities were made using 3C 48 for a few days during March-May 87. These are shown in Table 4.

13 On-going Expansion of the Thaltej Telescope

Since mid-1987, an Indo-US cooperative project on IPS has been launched between PRL and NOAA, Boulder. Under this project near real-time solar wind velocities will be measured using microprocessor-based digital data acquisition system and modems with dedicated telephone lines connecting the three sites.

In addition, IPS imaging of the interplanetary medium using scintillations of a large number of radio sources around the sun will be made. For this purpose, the IPS telescope at Thaltej is undergoing enlargement of its antenna array to 20,000 sq. m which will be used in conjunction with 32 double-channel receivers with provision of continuously monitoring scintillating flux of hundreds of radio galaxies. Such daily maps of plasma turbulence will enable study of day-to-day movements of turbulent plasma clouds in the 3-dimensional space in the IPM. These so-called 'g-maps' of large-scale variations of plasma density in the solar wind are known[6] to be related to heliospheric disturbances which emanate from the sun and sometimes engulf the earth, where they produce geomagnetic storms and associated ionospheric effects. Recently, this technique has enabled detection of a large number of solar disturbances, which, when traced back to the proximity of the sun, enable location of their origin.

Acknowledgement

The authors express their sincere gratitude to Prof. R K Varma for his support to this work. They thank all the staff members of the Radio Astronomy group for their valuable assistance to the IPS project. Financial support to this project came from the Departments of Space and Science & Technology, Government of India.

References

1 Salpeter E E, *Astrophys J (USA)*, 147 (1967) 433.
2 Readhead A C S, *Mon Not R Astron Soc (GB)*, 155 (1971) 185.
3 Duffett-Smith P J, *The regular sizes of radio sources at low frequencies*, PhD thesis, Cambridge University, Cambridge, 1976.
4 Readhead A C S & Hewish A, *Mem R Astron Soc, (GB)* 78 (1974) 1.
5 Kraus J D, *Radio Astronomy* (McGraw-Hill, (New York) 1966.
6 Gapper G R, Hewish A, Purvis A & Duffett-Smith P J, *Nature (GB)*, 296 (1982) 633.
7 Hewish A & Duffett-Smith P J, *Planet. Space Sci (GB)*, 35 (1987) 487.
8 Alurkar S K, Bhonsle R V, Sharma R, Bobra A D, Sohan Lal, Nirman N S, Venat P & Sethia G, *J Inst Electron Telecom Engrs*, 28 (1982) 577.
9 Bobra A D, Achari C K V & Ali H T, *PRL Tech Note (India)*, TN-86-57 (1986).
10 Bobra A D, Selvaraj M, Alurkar S K & Bhonsle R V, *J Inst Electron Telecom Engrs (India)*, 27 (1981) 569.
11 Armstrong J W & Coles W A, *J Geophys Res (USA)*, 77 (1972) 4602.
12 Coles W A & Kaufman J J, *Radio Sci (USA)*, 13 (1978) 591.